Available online at www.sciencedirect.com
ScienceDirect
Applied Surface Science 252 (2006) 7442–7448
applied surface science
www.elsevier.com/locate/apsusc

Growth of ZnO thin films on *c*-plane Al_2O_3 by molecular beam epitaxy using ozone as an oxygen source

Y.W. Heo [a], K. Ip [a], S.J. Pearton [a], D.P. Norton [a,*], J.D. Budai [b]

[a] *Department of Materials Science and Engineering, University of Florida, 106 Rhines Hall, P.O. Box 116400, Gainesville, FL 32611, USA*
[b] *Oak Ridge National Laboratory, Oak Ridge, TN 37831, USA*

Received 14 June 2005; accepted 31 August 2005
Available online 30 January 2006

Abstract

The growth of *c*-axis oriented ZnO thin films on *c*-plane Al_2O_3 via molecular beam epitaxy (MBE) using dilute ozone (O_3) as an oxygen source was investigated. Four-circle X-ray diffraction (XRD) indicates that films grown at 350 °C are epitaxial with respect to the substrate, but with a broad in-plane and out-of-plane mosaic. The films were highly conductive and n-type. Epitaxial film growth required relatively high Zn flux and O_3/O_2 pressure. The growth rate decreased rapidly as growth temperature was increased above 350 °C. The drop in growth rate with temperature reflects the low sticking coefficient of Zn at moderately high temperatures and limited ozone flux for the oxidation of the Zn metal. Characterization of the films included atomic force microscopy (AFM), X-ray diffraction, photoluminescence, and Hall measurements. These results show that molecular beam epitaxy of ZnO using ozone is rate limited by the ozone flux for growth temperatures above 350 °C.
© 2005 Elsevier B.V. All rights reserved.

Keywords: Zinc oxide; Semiconductors; Oxides; Molecular beam epitaxy

1. Introduction

In recent years, significant attention has been focused on the growth of ZnO thin films. This material is used for acoustic wave devices, varistors, gas sensors, piezoelectric transducers, transparent electrodes, and transparent thin film transistors [1–8]. It is an n-type direct bandgap (3.37 eV) semiconductor having a large exciton binding energy (60 meV) [9]. It has a hexagonal wurtzite crystal structure with $a = 0.32$ nm and $c = 0.512$ nm. It is naturally an n-type semiconductor because deviations from stoichiometry result in intrinsic donor defects, such as O vacancies (V_O) and Zn interstitials (Zn_i) [10]. In general, the selection of the oxygen source for oxide film growth plays an important role in determining the properties, including crystallinity, electrical transport, and optical characteristics [11,12]. Epitaxial ZnO thin films have been grown by

* Corresponding author. Tel.: +1 352 846 0525; fax: +1 352 846 1182.
E-mail address: dnort@mse.ufl.edu (D.P. Norton).

0169-4332/$ – see front matter © 2005 Elsevier B.V. All rights reserved.
doi:10.1016/j.apsusc.2005.08.094

numerous methods, including chemical vapor deposition (CVD), RF sputtering, pulsed laser deposition (PLD), and molecular beam epitaxy (MBE) [13–16]. For MBE growth, the high vapor pressure of Zn metal along with the limited kinetics of Zn oxidation in molecular oxygen (O_2) makes the use of highly oxidizing species necessary [11,12,17–19]. One source of reactive oxygen used in oxide film growth is atomic oxygen that is obtained by employing a plasma discharge. Significant work has focused on the MBE growth of ZnO epitaxial films using atomic oxygen [20–24], yielding films with electron mobility as high as 145 $cm^2/(V\ s)$ [23]. However, maintaining an oxygen plasma in an MBE environment can be limiting in terms of required hardware and total working pressure. Therefore, research into alternative oxidation sources is useful. For the growth of many oxides, ozone (O_3) has proven to be effective. The use of ozone precludes the need for a plasma source in the deposition system [25]. There have been limited investigations into the growth of ZnO using ozone, with the only published report focusing on polycrystalline ZnO deposition on Si [26]. In the present work, the epitaxial growth of ZnO thin films on sapphire using ozone in molecular beam epitaxy is reported.

2. Experimental details

The growth experiments were performed using a conventional MBE system. *c*-Plane Al_2O_3 wafers were used as substrates. Prior to film growth, the (0 0 0 1) Al_2O_3 substrates were cleaned with trichloroethylene, acetone, and methanol. Growth temperatures investigated for ZnO growth on *c*-plane Al_2O_3 ranged from T_g = 200 °C to 500 °C. The background base pressure of the growth chamber was $\sim 5 \times 10^{-8}$ mbar. An ozone/oxygen mixture was used as the oxidizing source. A nitrogen-free plasma discharge ozone generator was used to generate an O_3/O_2 mixture with ozone content in the order of 1–3%. No effort was made to separate the molecular oxygen from the ozone. The flux of Zn was provided by Knudsen effusion cells using high purity Zn metal (99.9999%) as the source. Zn and O_2/O_3 partial pressures were determined via a nude ionization gauge that was placed close to the substrate position prior to growth. The beam pressure of the O_3/O_2 mixture could be varied from 5×10^{-6} mbar to 5×10^{-4} mbar, yielding an O_3 partial pressure of 5×10^{-8} mbar to 5×10^{-6} mbar. Gas flow was controlled by a leak valve between the ozone generator and the chamber. The Zn pressure was varied between 5×10^{-7} mbar and 5×10^{-6} mbar. After growth, the samples were cooled to room temperature while maintaining the O_3/O_2 growth pressure. Surface profilometry across a film step was used to determine film thickness. The properties of the ZnO thin films were measured as a function of Zn flux, ozone flux, and growth temperature. The film properties were examined using atomic force microscopy (AFM), X-ray diffraction (XRD), photoluminescence, and Hall measurement.

3. Results and discussion

Initial film growth experiments investigated the possible MBE growth of ZnO with molecular oxygen only. At low substrate temperature, Zn metal was deposited but no ZnO was formed. As the deposition temperature was increased, no deposition occurred. In particular, the growth of ZnO using molecular oxygen was not observed under any conditions. However, employing the dilute O_3/O_2 mixture yielded ZnO film growth. Fig. 1 shows the growth rate of ZnO as a function of growth temperature for a Zn pressure of 2×10^{-6} mbar and an O_3/O_2 pressure of 5×10^{-4} mbar. The growth rate is relatively low and is measured to be approximately 50 nm/h for

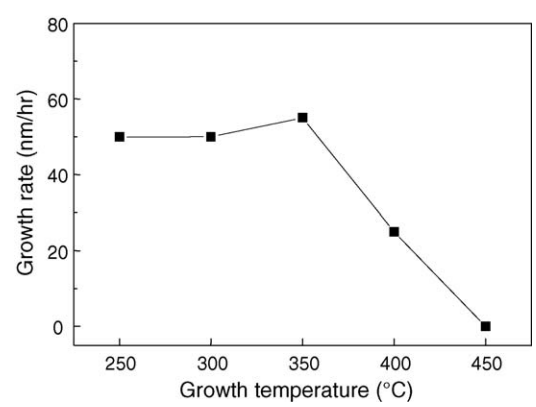

Fig. 1. Growth rate of ZnO grown on *c*-plane Al_2O_3 as a function of growth temperature with a Zn pressure of 2×10^{-6} mbar and O_3/O_2 pressure of 5×10^{-4} mbar.

temperatures up to 350 °C. Note that the O_3/O_2 flux rate was relatively high in order to achieve this modest growth rate. For growth temperature greater than 350 °C, the rate dramatically decreased. In fact, for growth temperatures above 450 °C, continuous films were not realized. An increase in growth temperature causes a decrease of the sticking coefficient of Zn on the Al_2O_3 substrate which, subsequently, causes a decrease in the growth rate, even though the reactivity between Zn and the oxygen source is expected to increase with growth temperature. It is also possible that decomposition of ZnO at the surface plays a role in the lack of film growth under these conditions. Note that there was no growth under any conditions when only O_2 was used as the oxygen source. This directly reflects the relatively high dissociation energy of molecular oxygen, which is in the order of 5.2 eV. In contrast, ozone decomposes exothermically, with a heat of decomposition around 1.69 eV/molecule [27]. At substrate temperatures sufficiently high to drive the reaction between O_2 and the Zn metal and form ZnO, the sticking coefficient for Zn is too low to sustain a surface reaction with O_2 on the Al_2O_3 surface. At temperatures greater than 350 °C, the drop in deposition rate reflects the high vapor pressure of Zn metal, which is in the order of 10^{-2} Torr, limiting surface collisions with ozone, as well as the decomposition of ZnO at the surface.

For film growth at the substrate temperature of 350 °C, the dependence of ZnO thin film crystallinity on Zn and oxygen flux was also investigated. If ZnO growth is limited by oxidation as suggested in the above discussion, the crystallinity should be a strong function of Zn flux and O_2/O_3 partial pressure. Formation of stoichiometric ZnO requires high flux of both Zn and the oxidizing species. Fig. 2 shows the X-ray diffraction patterns for films deposited at 350 °C under various Zn and O_3/O_2 flux rates. As shown in the figure, the growth of ZnO was not observed for a Zn pressure less than 2×10^{-7} mbar at a growth temperature of 350 °C. The highest (0 0 0 2) XRD peak intensity for the *c*-axis oriented ZnO films was observed with a Zn pressure of 2×10^{-6} mbar and an O_3/O_2 pressure of 5×10^{-4} mbar. This was the highest reactant flux investigated in this study, suggesting that growth is very much limited by ZnO formation at the substrate surface. In addition, the crystallinity of ZnO films grown at different temperatures was also examined. Fig. 3 shows the XRD patterns of ZnO films deposited on the *c*-plane Al_2O_3 at different growth temperatures with a Zn pressure of 2×10^{-6} mbar and an O_3/O_2 pressure of 5×10^{-4} mbar. The intensity of the (0 0 0 2) peak increases with growth temperature up to 350 °C, and then decreases for higher temperature. The ZnO (0 0 0 2) peak disappears at growth temperature of 450 °C. This behavior differs from molecular beam epitaxy grown ZnO films using a high flux of atomic

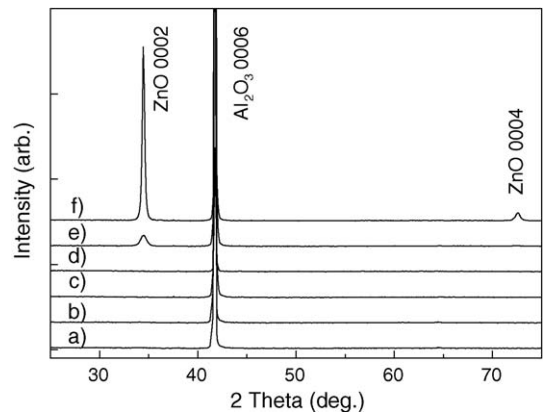

Fig. 2. XRD patterns of ZnO grown on sapphire (0 0 1) at 350 °C growth temperature as a function of Zn and O_3/O_2 pressures: (a) Zn of 2×10^{-7} mbar and O_3/O_2 of 5×10^{-6} mbar, (b) Zn of 2×10^{-7} mbar and O_3/O_2 of 5×10^{-5} mbar, (c) Zn of 5×10^{-7} mbar and O_3/O_2 of 5×10^{-4} mbar, (d) Zn of 2×10^{-6} mbar and O_3/O_2 of 5×10^{-6} mbar, (e) Zn of 2×10^{-6} mbar and O_3/O_2 of 5×10^{-5} mbar, and (f) Zn of 5×10^{-6} mbar and O_3/O_2 of 5×10^{-4} mbar.

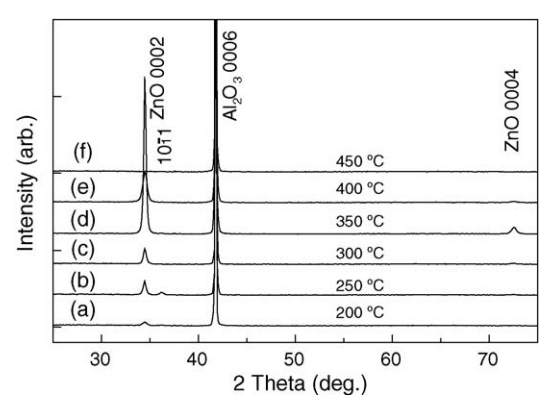

Fig. 3. XRD pattern of ZnO grown on sapphire (0 0 1) with a Zn pressure of 2×10^{-6} mbar and O_3/O_2 pressure of 5×10^{-4} mbar as a function of growth temperature (a) 200 °C, (b) 250 °C, (c) 300 °C, (d) 350 °C, (e) 400 °C, and (f) 450 °C.

oxygen [23] where growth is possible at much higher temperatures, thus reflecting the limitations on Zn oxidation for the ozone fluxes considered.

Despite the limited range of deposition conditions for ZnO formation, epitaxial ZnO films were realized. The epitaxial crystallinity of the films was confirmed using four-circle X-ray diffraction [28–30]. Fig. 4 shows the out-of-plane rocking curve (a) and in-plane ϕ-scan. The rocking curve through the (0 0 0 2) plane for the ZnO film grown at Zn pressure of 2×10^{-7} mbar and O_3/O_2 pressure of 5×10^{-4} mbar at 350 °C shown in Fig. 4(a) yields a full width half maximum (FWHM) of 1.2°, which is significantly broader compared to epitaxial films reported using atomic oxygen as the oxidation source [20–24]. Only the *c*-axis ZnO peaks are evident in a θ–2θ X-ray diffraction scan (not shown) along the surface normal. A high-resolution θ–2θ-scan through the (0 0 0 2) plane indicate that the 2θ FWHM is 0.26 °. A high-resolution scan through the (0 0 0 2) peak yields a

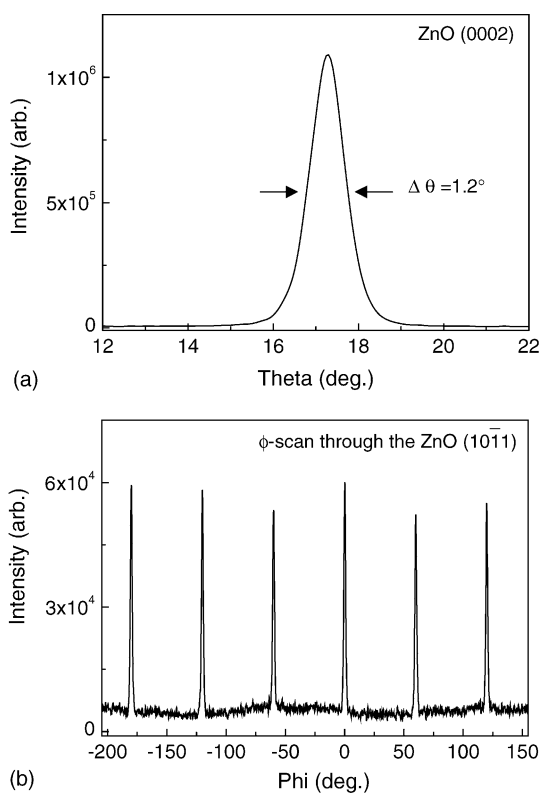

Fig. 4. (a) Rocking curve through (0 0 0 2) and (b) ϕ-scans for (1 0 $\bar{1}$ 1) plane of ZnO grown on *c*-plane Al_2O_3.

c-axis lattice parameter of 5.1948 Å, which is slightly smaller than the bulk value. ϕ-Scans through the ZnO (1 0 $\bar{1}$ 1) plane in Fig. 4(b) show in-plane alignment with $\Delta\phi = 1.6°$. The six-fold symmetry of the peaks in the ϕ-scan confirms that the hexagonal film is epitaxial [28–30]. Note that there is a 30° rotation between the in-plane ZnO and Al_2O_3 direction, determined by indexing the substrate in-plane axes relative to the ZnO peaks. This rotation is due to the 18% of lattice mismatch between film and substrate. The X-ray diffraction rocking curves for the films grown with ozone are somewhat broader than that seen in MBE films grown at higher temperatures using the plasma source. Again, this points to the oxidation of the Zn metal cation as a limiting factor in the growth of ZnO films.

The surface morphology of the ZnO film was measured using atomic force microscopy measurements. AFM measurement was performed in air using a Nanoscope III. All samples were scanned over a 1 μm × 1 μm area. In Fig. 5, the AFM images for ZnO films grown on sapphire at various temperatures are shown. A Zn pressure of 2×10^{-6} mbar and O_3/O_2 pressure of 5×10^{-4} mbar were employed during the growth. As the temperature increased from 200 °C, the roughness increased, reflecting an increase in ZnO grain size for growth temperatures up to 350 °C. At 450 °C growth temperature, the nucleation of ZnO decreased rapidly, with little or no ZnO film growth occurring. This was consistent with the XRD and growth rate behavior discussed earlier.

In addition to growth kinetics and crystallinity, the optical properties of these MBE-grown ZnO films using ozone were characterized using photoluminescence at room temperature. Photoluminescence spectra for films grown with a Zn pressure of 2×10^{-6} mbar and ozone pressure of 5×10^{-4} mbar mbar at a growth temperature of 350 °C were measured using a He–Cd laser (325 nm). The power density was 1 W/cm^2. A 0.3 m scanning grating monochromator with a Peltier-cooled GaAs photomultiplier was utilized. Fig. 6 shows the spectrum indicating a near band-edge emission at 3.30 eV for the film. The photoluminescent properties of ZnO typically reflect the intrinsic direct bandgap, a strongly-bound exciton state, and gap states due to point defects [31–34]. The strong room temperature near band-edge UV photoluminescence peak at

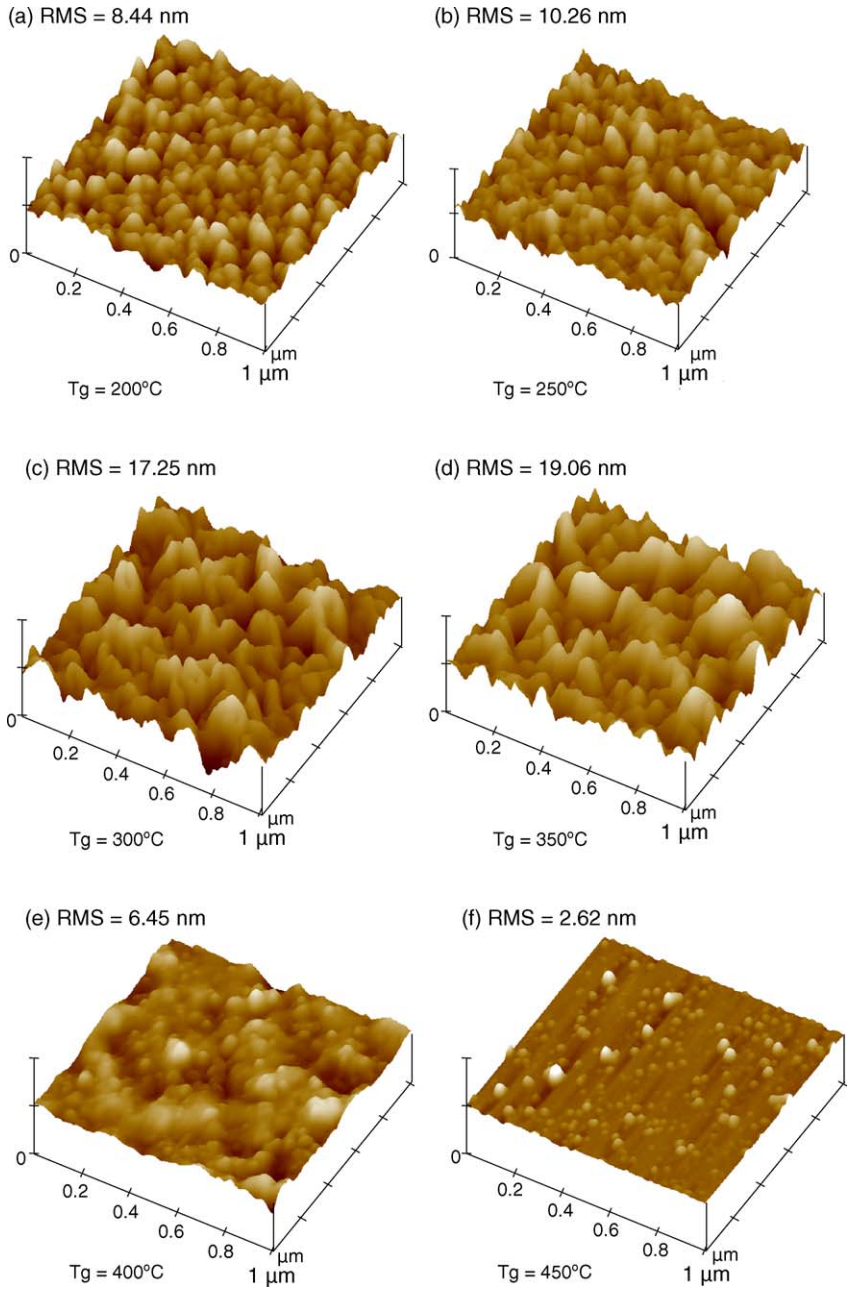

Fig. 5. AFM images of ZnO grown on sapphire with a Zn pressure of 2×10^{-6} mbar and O_3/O_2 pressure of 5×10^{-4} mbar as a function of growth temperature (a) 200 °C, (b) 250 °C, (c) 300 °C, (d) 350 °C, (e) 400 °C, and (f) 450 °C.

~3.2 eV is attributed to an exciton state, as the exciton binding energy is in the order of 60 meV [35]. In addition, visible emission is also observed due to defect states. In particular, broadband orange-red emission is seen at 1.9 eV and blue emission at 2.73 eV. The blue-green emission, centered at around 500 nm in wavelength, has been explained within the context of transitions involving self-activated centers

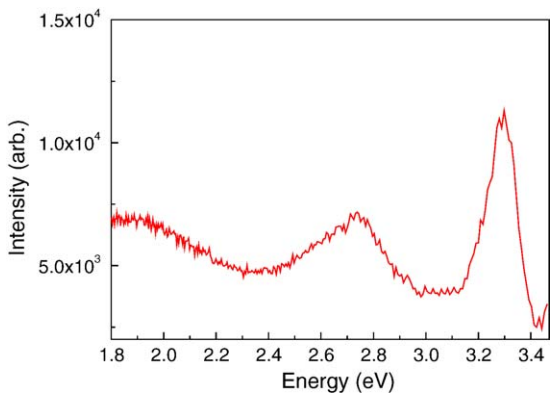

Fig. 6. Photoluminescence spectrum at room temperature of ZnO grown on sapphire with a Zn pressure of 2×10^{-6} mbar and O_3/O_2 pressure of 5×10^{-4} mbar at 350 °C growth temperature.

formed by a doubly ionized zinc vacancy and an ionized interstitial Zn^+ [34], oxygen vacancies [36–39], donor–acceptor pair recombination involving an impurity acceptor [40], and/or interstitial O [41–43]. The broad orange-red photoluminescence emission at ~1.9 eV has been observed in other ZnO film materials and has been assigned to defect states as well.

The carrier concentrations of these films were measured using Hall measurements. Fig. 7 shows the carrier concentration and resistivity of ZnO films grown on sapphire with a Zn pressure of 2×10^{-6} mbar and ozone pressure of 5×10^{-4} mbar as a function of growth temperature. Note that the carrier density was high in all samples relative to films grown using a

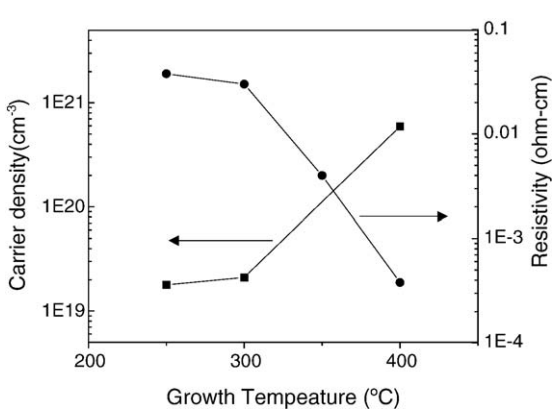

Fig. 7. Carrier concentration and resistivity of ZnO grown on sapphire as a function of growth temperature with a Zn pressure of 2×10^{-6} mbar and O_3/O_2 pressure of 5×10^{-4} mbar.

plasma source. Interestingly, the carrier concentration increased and resistivity decreased with the growth in temperature. Assuming that the films grown at low temperatures are oxygen deficient, one might anticipate higher carrier densities at the low growth temperatures.

In conclusion, the growth of ZnO thin films on *c*-plane Al_2O_3 via molecular beam epitaxy using ozone as an oxygen source was investigated. Epitaxial growth required high Zn and O_3/O_2 flux rates, with a limited temperature range for film growth. For the accessible O_3 flux rates, ZnO films grown at 350 °C using ozone (O_3/O_2) were highly conductive and n-type. At the higher temperatures, ZnO nanoscale island form, but do not appear to coalesce.

Acknowledgement

This work was supported by the Army Research Office.

References

[1] H. Nishiyama, N. Saito, H. Chou, K. Sato, Y. Inoue, Surf. Sci. 433–435 (1999) 525.
[2] Y.P. Wang, W.I. Lee, T.Y. Tseng, Appl. Phys. Lett. 69 (1996) 1807.
[3] W.P. Kang, C.K. Kim, Sens. Actuators B 13–14 (1993) 682.
[4] F. Paraguay D., M. Miki-Yoshida, J. Morales, J. Solis, W. Estrada, Thin Solid Films 373 (2000) 137.
[5] C.R. Wuethrich, C.A.P. Muller, G.R. Fox, H.G. Limberger, Sens. Actuators A 66 (1998) 114.
[6] S. Major, S. Kumar, M. Bhatnagar, K.L. Chopra, Appl. Phys. Lett. 49 (1986) 394.
[7] S. Masuda, K. Kitamura, Y. Okumura, S. Miyatake, H. Tabata, T. Kawai, J. Appl. Phys. 93 (2003) 1624.
[8] P.F. Carcia, R.S. McLean, M.H. Reilly, G. Nunes Jr., Appl. Phys. Lett. 82 (2003) 1117.
[9] D.C. Look, J.W. Hemsky, J.R. Sizelove, Phys. Rev. Lett. 82 (1999) 2552.
[10] D.C. Look, Mater. Sci. Eng. B 80 (2001) 383.
[11] S.A. Chambers, Surf. Sci. Rep. 39 (2000) 105.
[12] Y. Adachi, H. Ryouken, I. Sakaguchi, N. Ohashi, H. Haneda, T. Takenaka, Key Eng. Mater. 248 (2003) 83.
[13] K. Haga, M. Kamidaira, Y. Kashiwaba, T. Sekiguchi, H. Watanabe, J. Cryst. Growth 214 (2000) 77.
[14] R. Ondo-Ndong, G. Ferblantier, M. Al Kalfioui, A. Boyer, A. Foucaran, J. Cryst. Growth 255 (2003) 130.
[15] Y.W. Heo, S.J. Park, K. Ip, S.J. Pearton, D.P. Norton, Appl. Phys. Lett. 83 (2003) 1128.
[16] K. Sakurai, M. Kanehiro, K. Nakahara, T. Tanabe, S. Fujita, Fujita F.S., J. Cryst. Growth 214–215 (2000) 92.
[17] J.A. Rodriguez, J. Hrbek, J. Vac. Sci. Technol. A 12 (1994) 2140.

[18] R.I. Bickley, L.P. Metcalfe, J. Chem. Soc., Faraday Trans. I 74 (1978) 869.
[19] A. Krozer, B. Kasemo, Surf. Sci. 97 (1980) L339.
[20] Setiawan, Z. Vashaei, W. Meoung, T. Yao, H. Kato, M. Sano, K. Miyamoto, I. Yonenaga, J. Hang, J. Appl. Phys. 96 (2004) 3763.
[21] J.F. Yan, Y.M. Lu, Y.C. Liu, H.W. Liang, B.H. Li, D.Z. Shen, J.Y. Zhang, X.W. Fan, J. Cryst. Growth 266 (2004) 505.
[22] M. Fujita, N. Kawamoto, M. Sasajima, Y. Horikoshi, J. Vac. Sci. Technol. B (Microelectron. Nanometer Struct.) 22 (2004) 1484.
[23] H. Kato, M. Sano, K. Miyamoto, T. Yao, J. Cryst. Growth 265 (2004) 375.
[24] C. Morhain, M. Teisseire-Doninelli, S. Vezian, C. Deparis, P. Lorenzini, F. Raymond, J. Guion, G. Neu, Phys. Status Solidi B 241 (2004) 631.
[25] J.B. Kim, K. Chakrabarti, J.H. Lee, K.-Y. Oh, C. Lee, Mater. Chem. Phys. 78 (2003) 733.
[26] M. Fujita, N. Kawamoto, T. Tatsumi, K. Yamagishi, Y. Horikoshi, Jpn. J. Appl. Phys., Part 1 42 (2003) 67 (regular papers, short notes and review papers).
[27] A. Mills, S.-K. Lee, A. Lepre, J. Photochem. Photobiol. A 155 (2003) 199.
[28] A. Perrin, M. Guilloux-Viry, X. Castel, C. Le Paven-Thivet, Microelectron. J. 27 (1996) 343.
[29] C.R. Wie, Mater. Sci. Eng. R R13 (1994) 1.
[30] M. Halliwell, Microscopy of semiconducting materials, in: Proceedings of Royal Microscopy Society Conference, 1993, pp. 555–562.
[31] J. Gutowski, N. Presser, I. Broser, Phys. Rev. B 38 (1988) 9746.
[32] S. Bethke, H. Pan, B.W. Wessels, Appl. Phys. Lett. 52 (1988) 138.
[33] B.J. Jin, S.H. Bae, S.Y. Lee, S. Im, Mater. Sci. Eng. B 71 (2000) 301.
[34] B.J. Jin, S. Im, S.Y. Lee, Thin Solid Films 366 (2000) 107.
[35] D.M. Bagnall, Y.F. Chen, M.Y. Shen, Z. Zhu, T. Goto, T. Yao, J. Cryst. Growth 184–185 (1998) 605.
[36] E.G. Bylander, J. Appl. Phys. 49 (1978) 1188.
[37] N. Riehl, O. Ortman, Z. Electrochem. 60 (1952) 149.
[38] F.A. Kröger, H.J. Vink, J. Chem. Phys. 22 (1954) 250.
[39] Y. Prosanov, A.A. Politov, Inorg. Mater. 31 (1995) 663.
[40] N.Y. Garces, L. Wang, L. Bai, N.C. Giles, L.E. Halliburton, G. Cantwell, Appl. Phys. Lett. 81 (2002) 622.
[41] H.-J. Egelhaaf, D. Oelkrug, J. Cryst. Growth 161 (1996) 190.
[42] D. Hahn, R. Nink, Physik Cond. Mater. 3 (1965) 311.
[43] M. Liu, A.H. Kitai, P. Mascher, J. Lumin. 54 (1992) 35.